communications earth & environment

Article

A Nature Portfolio journal

https://doi.org/10.1038/s43247-025-02245-w

Unique (Al,Cu)-alloys discovered in a micrometeorite from Southern Italy

Giovanna Agrosì[1] ✉, Paola Manzari[2], Daniela Mele[1], Gioacchino Tempesta[1], Floriana Rizzo[1], Tiziano Catelani[3], Guangming Cheng[4], Nan Yao[4], Johan Villeneuve[5] & Luca Bindi[6] ✉

We report the discovery of a (Al,Cu)-bearing micrometeorite recovered at the top of Mt. Gariglione (Italy). The micrometeorite exhibits a highly vesicular scoriaceous structure characterized by broadly chondritic silicate-dominated composition (S-type) with relict phenocrystals of forsteritic olivine dispersed in a Ca-rich silicate glass with pyroxene composition, droplets of FeNi metal, oxides and sporadic Ni-rich sulphides embedded in a magnetite rim. The oxygen 3-isotope analyses give values close to the slope ~1 CCAM. A reduced assemblage of (Al,Cu)-alloys partially fills the open voids of the micrometeorite and shows variable compositions: from almost pure Cu up to Al-dominated phases with a predominance of khatyrkite, stolperite and unnamed Cu_3Al_2. Locally, small grains (about 1-2 μm in size) embedded in stolperite show a Fe-Si enrichment and are characterized by a long-range ordering resembling a quasicrystalline structure. This finding represents a unique natural quasicrystal approximant with composition $Al_{52}Cu_{31}Fe_{10}Si_7$.

Metallic (Al,Cu)-alloys are uncommon in both terrestrial and extraterrestrial materials mainly because Cu is a moderately volatile chalcophile element and Al is a highly refractory lithophile element. In extraterrestrial bodies, Al is mostly found in anorthite and spinel, while Cu is often present in sulphides. Thus, their coexistence opens intriguing scenarios on their origin and formation conditions. The first extraterrestrial body containing the exotic (Al,Cu)-alloys, named Khatyrka meteorite, was recovered in the Koryak Mountains, far eastern Russia[1–3]. Khatyrka is a CV3 carbonaceous chondritic breccia[4–8] and, besides crystalline (Al,Cu)-alloys, it contains the first naturally-occurring quasicrystals: icosahedrite, $Al_{63}Cu_{24}Fe_{13}$[1,9], decagonite, $Al_{71}Ni_{24}Fe_5$[10,11], and an unnamed *i*-phase II, $Al_{62}Cu_{31}Fe_7$[12,13]. Khatyrka is also characterized by high-pressure phases such as stishovite and ahrensite, which are sensitive of an impact-induced shock event[2,5]. A second micrometeorite with metallic (Al,Cu,Fe)-assemblages, and showing close similarities with Khatyrka was described from the Nubian desert, Sudan[14,15], and very recently a new chondritic micrometeorite from Congo shows the presence of this "exotic" alloys[16]. In both these cases, high-pressure phases are absent, and mainly due to the low Fe content in the alloys, they do not contain any quasicrystalline phases.

Here, we report the discovery of a new extraterrestrial object containing the exotic (Al,Cu)-alloys. The micrometeorite was found by an amateur micrometeorite hunter at the top of Mt. Gariglione (south Italy), about 65 km north of the city of Catanzaro (39° 7' 55" North, 16° 40' 12" East). In this sample, we document the first occurrence of a quaternary alloy with the $Al_{52}Cu_{31}Fe_{10}Si_7$ stoichiometry, where silicon, beside Al, Cu and Fe, is an essential component.

Results And Discussion

The sample, labelled FB-A1, consists of an elongated microspherule of about 500 μm in max diameter. It is dark grey with visible portions exhibiting metallic luster and shows a singular scoriaceous structure with vesicles and some protruding spherical metal particles (Fig. 1a). The morphological aspect of this micrometeorite seems to be optically very similar to that studied by Suttle et al.[14]. To optimize the investigation, preserving at first the integrity of the microspherule so as not to lose valuable information, the analyses have been carried out in a nondestructive way on the intact sample, using micro-Computed X-ray Tomography (μ-CT) and Scanning Electron Microscopy (SEM) equipped with an energy-dispersive spectrometer (EDS). Preliminary SEM-EDS analysis on the external surface revealed that most of the metallic portions (light grey back-scatter signal in Fig. 1b) correspond to (Al,Cu)-alloys. These metallic alloys form the protruding spherical particles and also smeared particles on the surface of microspherule (see Fig. S1). A magnetite rim partially covers the surface of microspherule (Fig. S2 and Table S4) and consists of an aggregation of dendritic crystals disseminated in a porous matrix of silicate glass also containing forsteritic olivine crystals, Fe-Ni droplets, and sporadic Fe-Ni

[1]Department of Earth and geoenvironmental sciences, University of Bari Aldo Moro, Bari, Italy. [2]Italian Spatial Agency, Centro Spaziale di Matera, Terlecchia, Matera, Italy. [3]Service Centre MEMA, University of Florence, Florence, Italy. [4]Princeton Materials Institute, Princeton University, Princeton, NJ, USA. [5]University of Lorraine, CNRS, CRPG, Nancy, France. [6]Department of Earth Sciences, University of Florence, Florence, Italy. ✉e-mail: giovanna.agrosi@uniba.it; luca.bindi@unifi.it

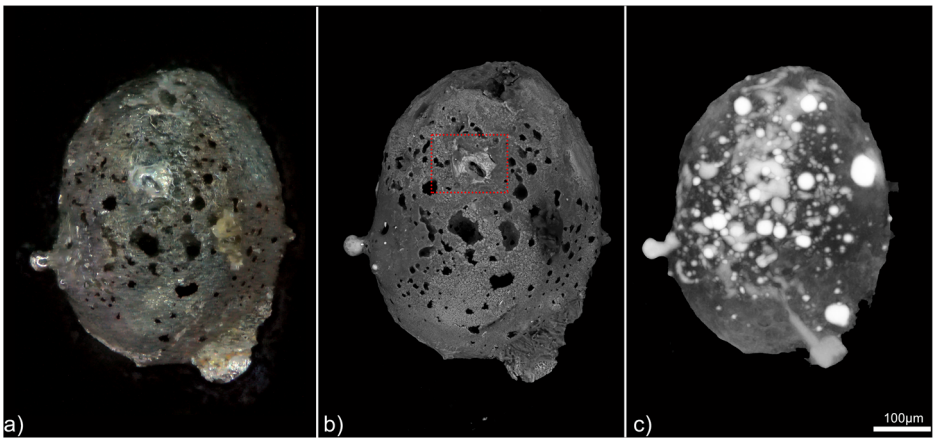

Fig. 1 | FB-A1 micrometeorite from Mt. Gargione (Italy). a Optical image (**b**) SEM-BSE image (the red rectangle marks the enlarged region shown in Fig. 1S); **c** micro-CT volume rendering (in light grey the Al-Cu alloys and as small bright droplets the Fe-Ni alloys disseminated in the whole volume).

sulfides. The µ-CT analyses reveal that the (Al,Cu)-alloys are dispersed not only on the surface of FB-A1 but also in its inner part (Fig. 1c). The 3D reconstruction obtained by µ-CT, which represents a very useful approach to obtain information about the spatial distribution and the relationships of mineralogical phases[17,18], shows that the interior of the spherule is enriched of (Al,Cu)- and (Fe,Ni)-alloys intermixed with silicates. The morphology of the (Al,Cu)-alloys varies from a sub-spherical form, which in some cases protruded on the surface of micrometeorite, to an irregular and elongated shape that intrudes the inner part of microspherule (Fig. 1c).

Electron microprobe analyses (EPMA), SEM and electron backscatter diffraction (EBSD) have been used for the subsequent, more in-depth investigations of the chemical and mineralogical composition of FB-A1, after polishing of one side of the microspherule.

The SEM Backscattered Electron (BSE) image of the polished surface shows an ellipsoidal shape with a micro-porphyritic texture, and a silicate-dominated composition (S-type)[19] with light grey contrasts corresponding to (Al, Cu)- and (Fe, Ni)-alloys and dark contrasts corresponding to vesicles and subspherical voids (Fig. 2). The bulk composition obtained by wide-beam analyses (see Table S1) is broadly chondritic and similar to that of Nubian desert[14,15] and Congo micrometeorites[16]. Moreover, these chemical data are characterized by a volatile depletion. Actually, the bulk composition is characterized by a total absence of Na and a very low content of S related to a near total degassing that occurred at high altitude during the atmospheric entry, as testified also by the presence of voids and vesicles. The BSE grey matrix consists of a Ca-rich silicate glass with pyroxene composition (En_{17}, Fs_{61}, Wo_{22}; Table S2) in which there are two types of olivine crystals: sub-rounded phenocrystals (up to 100 µm in size) and euhedral and in some cases skeletal dusty olivine crystals (<10 µm) dispersed in the mesostasis (Fig. 3a). The BSE images of both types of olivine show a brighter rim with respect to the core, suggesting a normal chemical zoning. In particular, the rounded phenocrystals exhibit a forsteritic core (Fo90%) surrounded by irregular outlines indicative of peripheral partial melting and recrystallization likely occurred by thermal stress during atmospheric entry[19–21]. The composition of the rim appears significantly enriched in Fe (Fo70%), even if some micro-phenocrystals also exhibit reverse zoning, suggesting complex redox reactions. Conversely, the size, morphology, and skeletal appearance of the dusty crystals of olivine indicate a rapid growth during cooling. Due to the small size of these olivines, it was only possible to determine the average composition (~Fo80%) (Table S2). The observed chemical and morphological features agree with the olivine crystals reported for the Nubian desert micrometeorite[14] whereas they differ from those observed for olivine in Grain126A of the Khatyrka meteorite (Fo50-56%[6]), which are more enriched in iron. As reported by Suttle et al.[14], the characteristics observed for the phenocrystals of olivine suggest that these phases represent unmelted relicts of forsterite, whereas the dusty olivines represent mesostasis products, formed by quench cooling during atmospheric entry. The thermal stress and redox reactions that occurred during the passage of the atmosphere also explain the formation of very tiny crystals of magnetite present mainly at the rim of the sample (Fig. 3b and Table S4), the droplets of (Fe, Ni)-alloy with variable stoichiometric ratios (Fig. 3b and Table S3), and the sporadic droplets of Ni-rich sulphides, as a droplet of almost pure heazlewoodite found in meteorite fusion crusts[22] (see Fig. 3d and Table S4). The chemical and mineralogical composition and the structure observed on FB-A1 are typical features of a chondritic micrometeorite, as suggested also by the similarity with a Nubian microspherule previously found[14]. Although spherical particle morphologies are particularly ambiguous since anthropogenic particulates, impact spherules, meteorite ablation spheres, airburst spherules[23], and even some small particles of volcanic dust may have similar morphologies, the observed depletion in Na and S and the magnetite rim supports further that FB-A1 is a micrometeorite, excluding meteorite ablation debris[22,24].

Actually, the presence of a magnetite-rim unequivocally distinguishes the fusion crust of micrometeorites and meteorites since this is developed during hypervelocity deceleration at high altitudes[25]. Nevertheless, to confirm the extraterrestrial nature of this particle and to determine the type of micrometeorite, oxygen isotopic analyses were also carried out, mainly on relict olivine crystals. The data obtained fall on (near) the CCAM line, indicating an affinity to carbonaceous chondrites of the CO-CV group (Fig. 4). The singularity of FB-A1, that needs to be explained, is the presence of the exotic metal alloys. If (Fe, Ni) alloys (see Table S3) exhibit rounded shapes similar to droplets, (Al, Cu)-alloys display irregular shapes on the polished surface and protruding particles on the micrometeorite's surface (Figs. 1, 2, 3a, c).

The (Al,Cu)-alloys exhibit different stoichiometries with a very low content of Fe (from 1.15 to 3.14 wt%) (see Table S5) and appear as an assemblage of domains and/or lamellae with variable compositions corresponding to the different scale of grey in the BSE images (Fig. 3c). They consist mainly of khatyrkite ($CuAl_2$) (darker grey) and stolperite (CuAl) (lighter grey) (Fig. 3c), as also revealed by EBSD (Fig. 5), even if there are also portions of nearly pure Al or near pure Cu, as well as tiny veins of a phase with a stoichiometry close to Cu_3Al_2 inside stolperite. The mineralogy at the metal/silicate interface is noteworthy. There is a thin rind of a Mg-Al-oxide surrounding the (Al,Cu)-alloys, likely a pure $MgAl_2O_4$ spinel (Fig. 6a, b), and small spherical droplets mostly iron in composition (Fig. 6b). These features are the same observed in Khatyrka[4] and in the micrometeorite from the Nubian desert[14] and are consistent with the formation processes previously proposed[6] involving the "thermite" reaction coupling the reduction of FeO and the oxidation of metallic Al.

The most remarkable portion of (Al,Cu)-alloy is reported in Fig. 6. The small grain has portions unusually enriched in Fe (dark grains of 1–2 µm located on the peripherical zone of stolperite in Fig. 6a) with a lower-Z than the stolperite-host. Electron microprobe (EMPA) analyses (Table S6 and S7) show the presence of conspicuous amounts of Fe and Si beside Cu and Al. Given the tiny size of the new phase, we paid

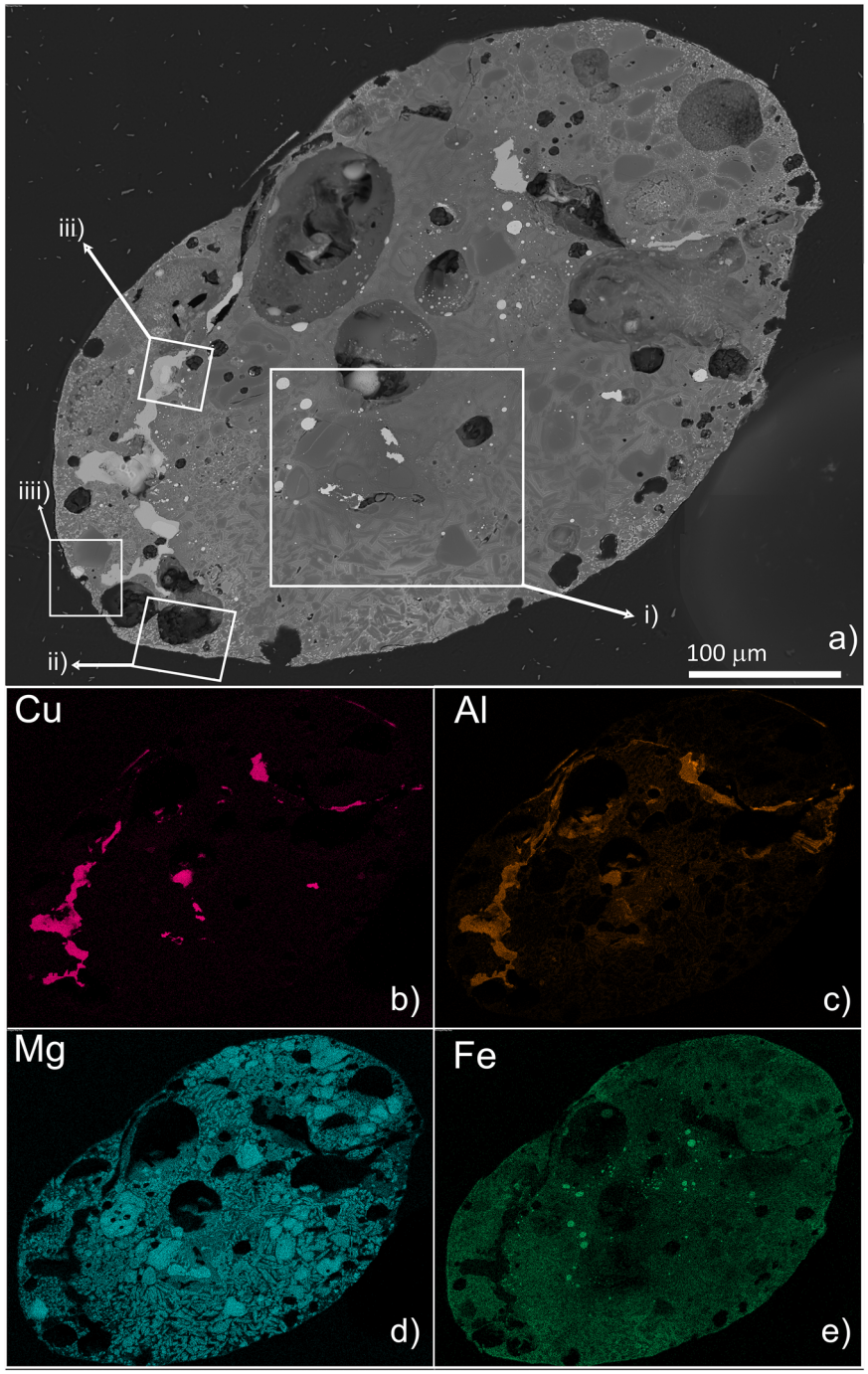

Fig. 2 | SEM images of FB-A1 polished surface and chemical mapping. a SEM-BSE image showing the polished surface. The (i), (ii), (iii), and (iv) rectangles indicate the regions enlarged in Fig. 3a–d, respectively. **b** X-ray chemical map of Cu; **c** X-ray chemical map of Al; **d** X-ray chemical map of Mg; **e** X-ray chemical map of Fe.

particular attention to contamination effects due to the silicate matrix. Silicon in the metallic phase, indeed, could come from the surrounding olivine. Considering that in the case of matrix contamination also, Mg (beside Si) should be present in the metal phase, particular care was devoted to the analysis of the spectra collected on single spots and line profiles (Fig. 6d). The analysis did not show any presence of Mg in the (Al, Cu, Fe, Si)-phase thus indicating that Si is an actual component of this new metallic alloy (see Table S7). The empirical formula (based on 100 atoms *pfu*) can be written as $Al_{51.7(6)}Cu_{30.8(9)}Fe_{10.3(4)}Si_{7.2(9)}$, ideally $Al_{52}Cu_{31}Fe_{10}Si_7$. EBSD data collected on these (Fe, Si)-rich portions revealed a pattern resembling an icosahedral symmetry (Fig. 6c). Nevertheless, the EBSD data, while suggesting a potential quasicrystal, could also be reasonably explained by an approximant periodic phase (Fig. 6c). Periodic approximant is an accepted technical term that refers to a crystalline solid with similar chemical composition to a quasicrystal, but whose atomic arrangement is slightly distorted so that the symmetry conforms to the conventional laws of three-dimensional crystallography. To shed light on the structure of $Al_{52}Cu_{31}Fe_{10}Si_7$, a Focused Ion Beam (FIB) lamella was extracted (Fig. 7) and studied by transmission electron microscopy (TEM). STEM-EDS analyses, acquired on different portions of the new metallic alloy, confirm the chemical composition found with the EMPA (Fig. 8). Electron diffraction data obtained from different grains of the (Al, Cu, Fe, Si)-alloy reveal that the phase is cubic, space group *Pm*-3, with $a \approx 12.4$ Å (Fig. 9a), closely matching the structure of the synthetic 1/1 $Al_{55}Si_7Cu_{25.5}Fe_{12.5}$ approximant (Fig. 9b)[26–28]. Noteworthy, an icosahedral phase with the same $Al_{55}Si_7Cu_{25.5}Fe_{12.5}$ stoichiometry has been described[26], and it was found that a relatively slow solidification would favour the formation of the quasicrystalline phase,

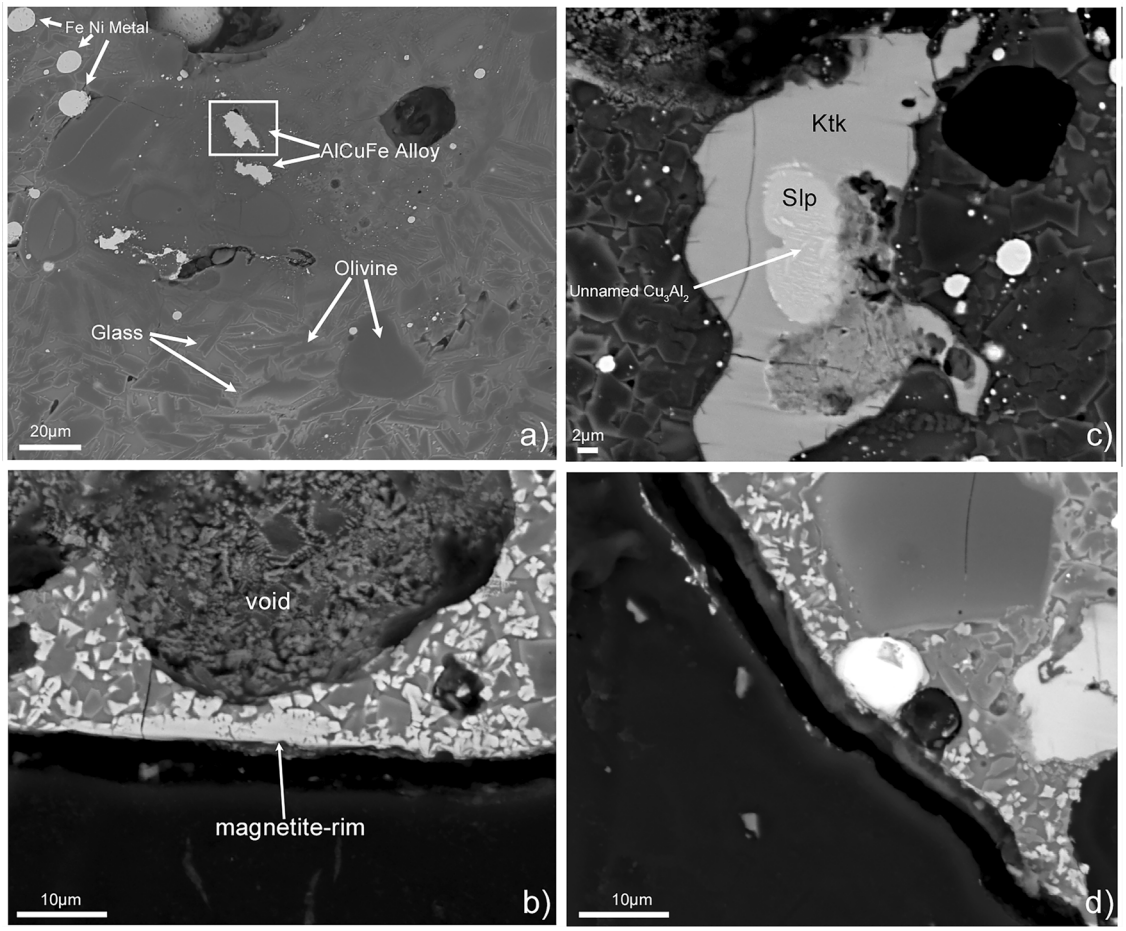

Fig. 3 | SEM-BSE images of FB-A1 polished surface. Showing the portions of FB-A1 highlighted as (i), (ii), (iii), and (iv) in Fig. 2a. **a** The (i) portion corresponding to the inner part of micrometeorite with rectangle enlarged in Fig. 5. **b** The (ii) portion corresponding to an enlarged particular of magnetite rim. **c** The (iii) portion of Al-Cu alloy. Ktk = khatyrkite, Slp = stolperite (note in stolperite the presence of lamellae with different scale of gray, corresponding to tiny brighter veins of Cu_3Al_2), (**d**) the (iv) portion with hzl: hezwooldite grain.

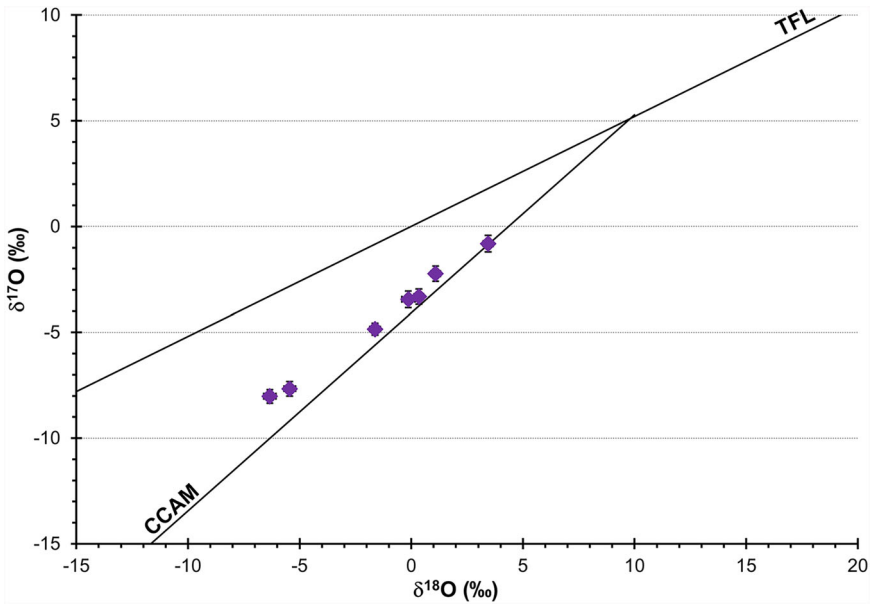

Fig. 4 | $\delta^{17}O$ versus $\delta^{18}O$ diagram. (values in ‰ versus V-SMOW) to discriminate terrestrial and extraterrestrial minerals. The plotted data were mainly taken on the relict olivine crystals of FB-A1 micrometeorite. The error bars fall under the diameter of each point analyses. The resulting oxygen isotope compositions lie along the line corresponding to anhydrous minerals in the CO or CV carbonaceous chondrites (the CCAM).

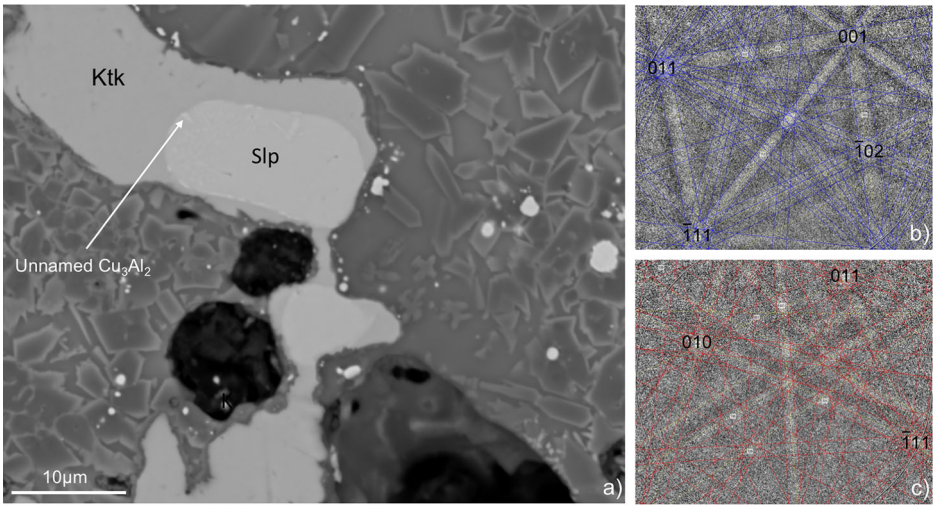

Fig. 5 | SEM-BSE image and EBSD patterns. **a** SEM-BSE image showing a portion of FB-A1 containing khatyrkite (Ktk), stolperite, (Slp), and tiny veins of Cu3Al2 inside stolperite; **b** EBSD pattern taken on stolperite (Slp) with mean angular deviation= 0.79; **c** EBSD pattern taken on khatyrkite (Ktk) with mean angular deviation = 0.87).

while higher quenching rates would trigger the conversion of the quasicrystal into the cubic approximant[29]. Consequently, the presence of the natural cubic approximant in the micrometeorite studied here might be sensitive to an increase in cooling rate during the crystallization.

The cubic $Al_{52}Cu_{31}Fe_{10}Si_7$ approximant reported here is the third reported in nature after the discovery of extraterrestrial proxidecagonite, $Al_{34}Ni_9Fe_2$[30], and terrestrial proxitwelvefoldite, $Pd_3Ni_4Te_8$[31]. The new approximant is close in composition to synthetic icosahedral and cubic 1/1 $Al_{55}Si_7Cu_{25.5}Fe_{12.5}$ approximant[27]. The slightly different Al/Cu ratio between the natural and synthetic phases is unsurprising. The difference between the product obtained in the laboratory and the natural phase could be linked to a kinetically stabilized composition, only preserved because of very rapid quench. This would imply that the new alloy described here would be thermodynamically unstable at any pressure and temperature. A similar (but even more evident) variation has been observed between icosahedrite ($Al_{63}Cu_{24}Fe_{13}$[9]); and *i*-phase II ($Al_{62}Cu_{31}Fe_7$[12]); and testifies how the shock generated in the collision among planetary bodies is responsible for a wider thermodynamic stability range of these metallic phases at high pressure[32,33].

Further studies on FB-A1 to shed light on the chondrite precursor, the mechanisms of formation of these peculiar phases and the thermodynamics of these exotic assemblages are currently in progress.

Conclusions

FB-A1 can be identified as a micrometeorite on the basis of the following evidence: the oxygen isotope ratios of the sample confirm its extraterrestrial origin, plotting close the CCAM line, moreover, the presence of an external magnetite rim, silicate portions dominated by olivine, glass and the presence of a high-Ni metal bead represent specific features that characterize micrometeorites[19,34]. Furthermore, the sub-spherical shape, the presence of unmelted olivines dispersed in Ca-rich silicate glass with pyroxene composition, the discontinuous magnetite rim and the highly porosity characterized by voids and vesicles, allow to classify FB-A1 as a specimen with intermediate features between those typically observed for cosmic spherules and those for scoriaceous micrometeorites with carbonaceous chondritic composition. The presence of (Al, Cu)-alloys, previously reported only in Khatyrka and in Sudan and more recently in Congo micrometeorites, represent exotic non-chondritic components, which likely formed after the initial host's accretion and were delivered most probably by an impact event[16]. In particular, in the study on the Congo micrometeorite an ureilite parent body has been suggested to be the most likely source for these (Al,Cu)-alloys[16].

In our case, the entire metallic assemblage and the newly described $Al_{52}Cu_{31}Fe_{10}Si_7$ alloy can be formed by an entirely uncontrolled mechanism, lasting perhaps a few minutes, yet resulting in almost identical to industrial artificial approximants/quasicrystals with similar composition.

The discovery of FB-A1 is an exceptionally rare finding, primarily due to the unusual composition of the particle. As it is well known, most micrometeorites consist predominantly of silicates, (Fe,Ni)-metals, and other elements commonly associated with extraterrestrial material. The presence of aluminium and copper in a micrometeorite is highly atypical because these elements are not abundant in natural cosmic dust sources, raising questions about its origin and formation processes.

One possible explanation for its rarity is that aluminium and copper are not typically stable in the high-temperature environments experienced during atmospheric entry. Most micrometeorites undergo significant melting and oxidation, leading to the loss or alteration of volatile and reactive elements. Aluminium, for instance, has a relatively low melting point compared to refractory materials like nickel, making it more susceptible to vaporization. Copper also oxidizes readily, forming compounds that may not survive the extreme thermal conditions of entry. Consequently, any micrometeorite containing these elements would need to originate from an unusual source, such as a highly differentiated planetary body, and survive the entry process largely intact[16].

Another factor contributing to the lack of similar discoveries in existing collections is the potential for misidentification or underreporting. Many large micrometeorite collections have been assembled based on established classification criteria that prioritize certain compositions and exclude others. Since (Al,Cu)-bearing particles do not fit the conventional profiles of extraterrestrial material, they may have been overlooked or dismissed as terrestrial contaminants during sample sorting.

Additionally, the formation and transport mechanisms of (Al,Cu)-micrometeorites remain unclear, which further complicates their identification. If these particles originate from a niche cosmic source, their flux to Earth may be exceptionally low, reducing the probability of their collection. Moreover, if they are particularly fragile or prone to alteration in Earth's environment, they may degrade before being recognized. This decreases the possibility that (Al,Cu)-rich micrometeorites can be found.

Ultimately, the rarity of (Al,Cu)-micrometeorites underscores the need for more comprehensive and unbiased searches in existing and future micrometeorite collections. Expanding classification criteria and applying more refined analytical methods may reveal previously unnoticed extraterrestrial particles with unconventional compositions, potentially offering new insights into the diversity of materials present in the cosmic dust influx to Earth.

Materials And Methods

Samples

The micrometeorite was provided by an Italian amateur collector to three of us (G.A., G.T., and P.M.). The collector reports that the fragment was found in 2002 during a collection of micrometeorites done by means of steel

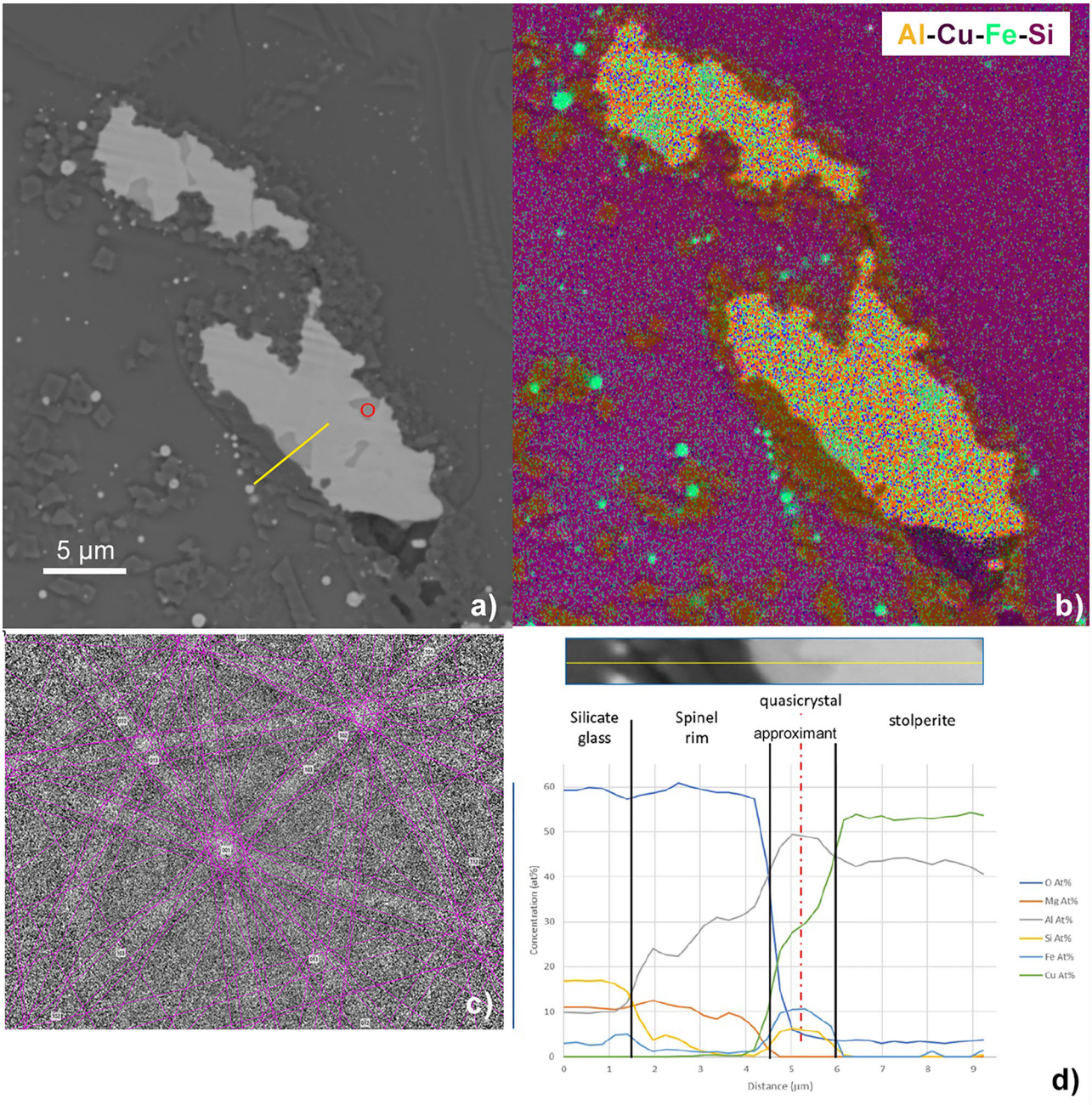

Fig. 6 | SEM-BSE image and EBSD patterns. a SEM BSE image of the rectangle highlighted in Fig. 3a. The bright phase is stolperite (with slightly variable Cu/Fe ratio), the dark phase is the new (Al, Cu, Fe, Si)-metallic alloy. The red spot indicates the point where the EBSD pattern was collected and the yellow line indicates the microanalyses traverse, **b** chemical mapping, **c** EBSD pattern taken on the red spot is matched with the cubic structure of the 1/1 approximant[22] with mean angle deviation = 0.81. **d** SEM-EDS microanalysis traverse taken along the yellow line of Fig. 5a.

funnels installed in isolated areas, away from any form of industrial contamination. The method of collection consists of equipping the bottom of the funnels with special filters able to retain material down to 10 µm. The filters are changed every two days and the material - fallen from the sky and located at the bottom of the steel funnels - is collected. The filters are then carefully checked under a binocular microscope. The micrometeorite of the current study attracted the attention of the amateur because of the unusual luster of the metallic phases present on the surface of the spherule, which seemed different than the classical (Fe,Ni)-metals. The micrometeorite was stored in his archive until a few months ago when he decided to send us this exotic spherule for further investigations. FB-A1 is now deposited in the collections of the Museo di Scienze della Terra of the University of Bari (Italy), registration number 19/nm.

After a preliminary and non-destructive check by SEM and a µ-CT study at the University of Bari (Italy), the sample was embedded in epoxy resin and polished (using diamond pastes) for the subsequent SEM and EPMA analyses carried out at the University of Florence (Italy), oxygen isotope analyses were carried out at CRPG-CNRS (Nancy, France) and, lastly, FIB-TEM investigations were performed at the Princeton University (USA).

Scanning Electron Microscopy

The SEM microscope used for preliminary and non-destructive check is Zeiss LEO, model EVO-50XVP, housed at the Department of Earth and Geo-environmental Sciences, University of Bari Aldo Moro (Italy), coupled with an X-max (80 mm2) energy dispersive (ED) Silicon drift Oxford

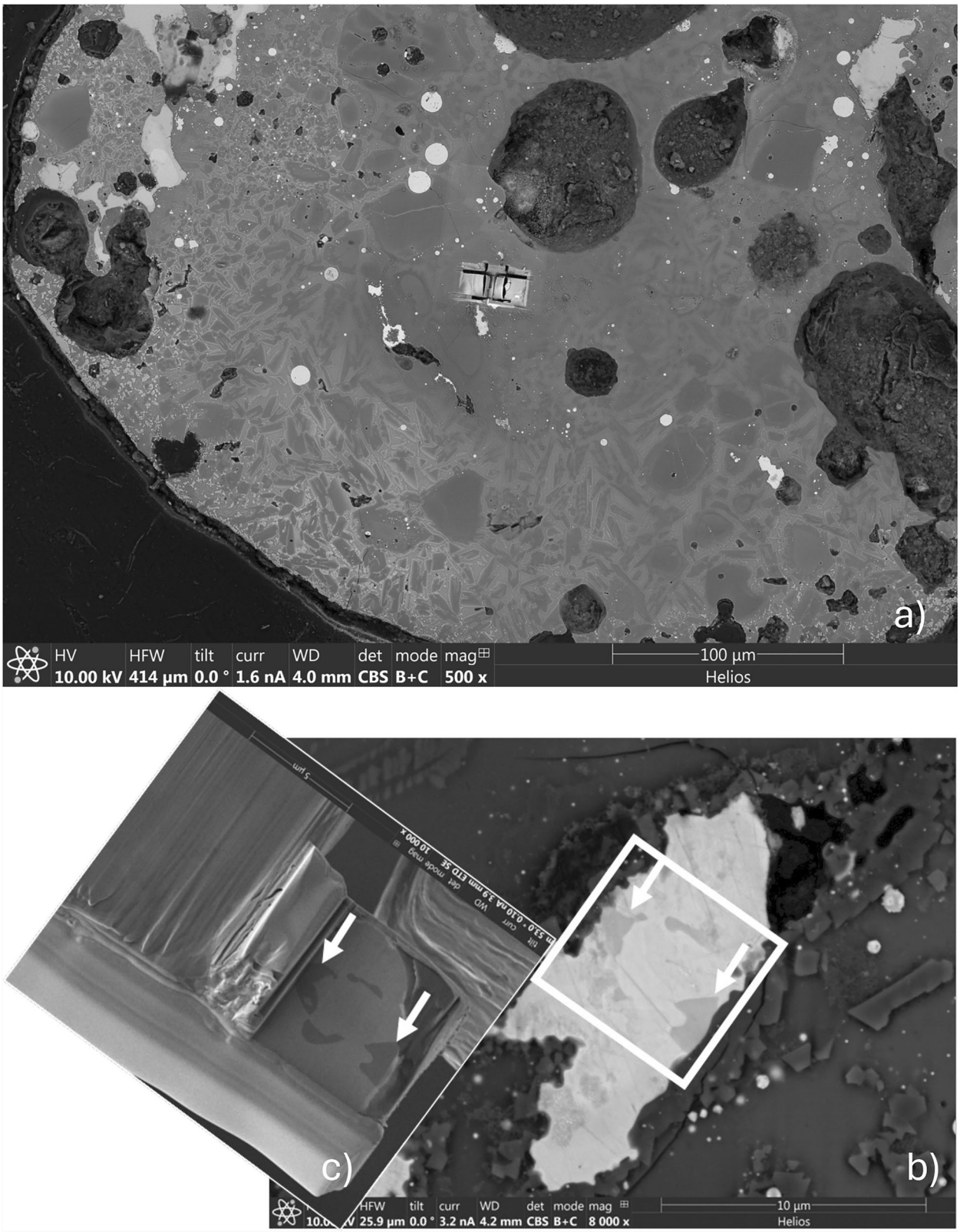

Fig. 7 | FIB lamella from FB-A1 micrometeorite. a SEM-BSE images showing the region where the FIB lamella was extracted; **b** STEM images of the grain where the FIB lamella was extracted; **c** FIB lamella. The white arrows indicate the dark regions corresponding to the (Al,Cu, Fe, Si)-alloy.

detector (Oxford Instruments) equipped with a Super Atmosphere Thin Window, operating at 15 kV accelerating potential and 500 pA probe current, 5 nm beam size and 8.5 mm working distance. It has secondary (SE) and backscattered electron (BSE) detectors.

The instrument used to analyze the polished surface of micrometeorite was a Zeiss EVO MA15 scanning electron microscope, housed at the Centre for Electron Microscopy and Microanalysis (MEMA) of the University of Florence (Italy), coupled with an Oxford UltimMax 40 energy-dispersive

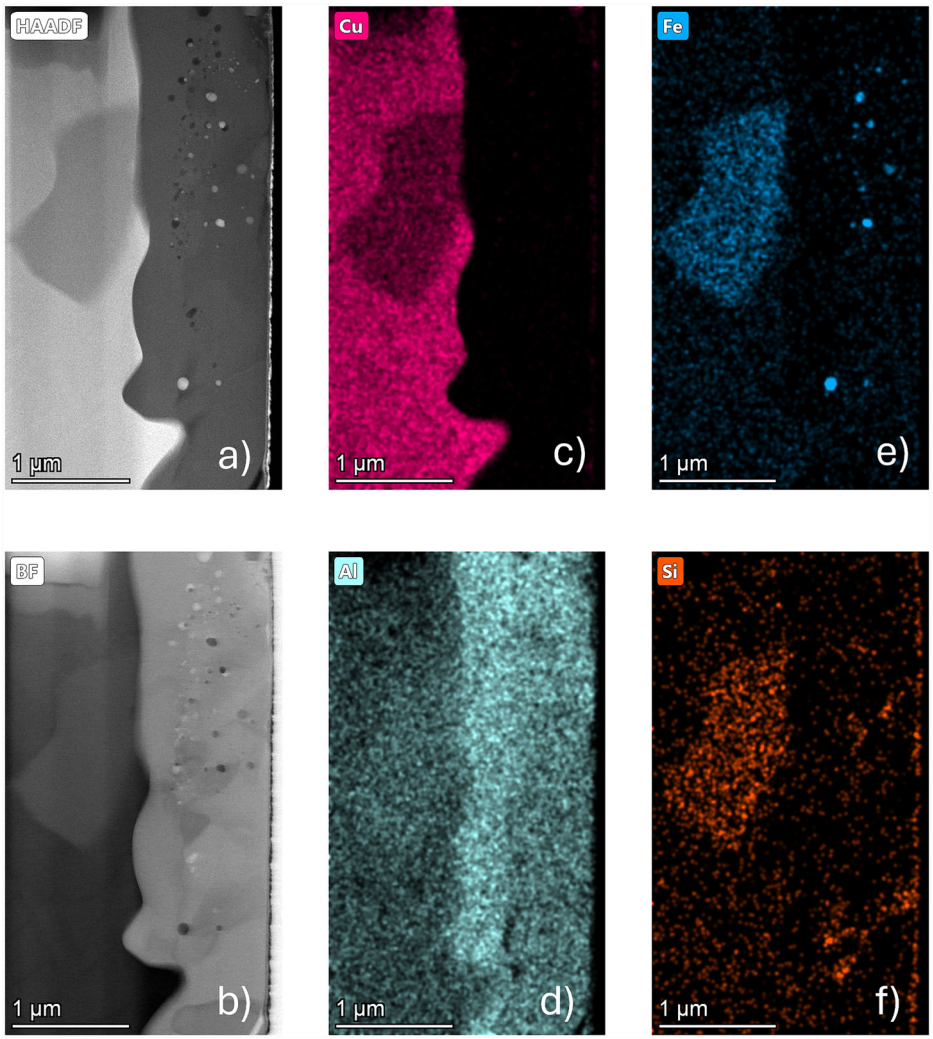

Fig. 8 | TEM analyses of FIB lamella. a HAADF image of a portion containing the (Al, Cu, Fe, Si)-alloy. The red spot indicates the point of acquisition of SAED and HR-image shown in Fig. 8. **b** BF image of the same region shown in (**a**). **c** STEM-EDS mapping of Cu; **d** STEM-EDS mapping of Al; **e** STEM-EDS mapping of Fe; **f** STEM-EDS mapping of Si.

spectrometer (EDS), operating at 15 kV accelerating potential and 700 pA nominal current in focused beam mode, for EDS mapping and spectra acquisition (30 seconds live time). For linescan analyses, the instrument was set up at 10 kV acceleration voltage and 500 pA nominal probe current (20 seconds dwell time for each point). The sample was sputter-coated with 30-nm-thick carbon film.

Electron backscatter diffraction

Analyses were performed using high-performance CMOS Oxford Symmetry S2 EBSD system working on a ZEISS EVO 15-MA SEM, operating at 15 kV and 9 nA nominal current in focused beam mode with a 70° tilted stage. EBSD patterns for phase identification and analysis were acquired with maximum pixel resolution (1244 × 1024). The cell constant was obtained by matching the experimental EBSD patterns to those of known synthetic phases. The sample was sputter-coated with 5 nm-thick carbon film.

Electron Microprobe

Quantitative analyses on the micrometeorite were carried out at the University of Florence (Italy), using a JEOL 8200 electron microprobe (WDS mode, 12 kV and 5 nA, focused beam). The focused electron beam is ~150 nm in diameter. Analyses were processed with the CITZAF correction procedure. The (Al,Cu,Fe,Si)-alloy was found to be homogeneous within analytical error. The standards used were Al metal, Si metal, Cu metal, and Fe metal. Seven point-analyses on different spots were collected. Ni, Ca and Mg were also analyzed using standards Ni metal, anorthite and forsterite, respectively. They were below detection limits: Ni 0.23 wt%, Ca 0.04%, Mg 0.06%.

Micro-computed X-ray Tomography

X-ray imaging was carried out with a Bruker SkyScan 1172 high-resolution µ-CT scanner equipped with a polychromatic microfocus X-ray tube. The cosmic spherule was scanned using a pixel size of 0.50 µm. A 79 kV X-ray source was used with a current of 131 µA. A total of 1127 absorption radiographs were acquired over a 360 rotation with an angular step of 0.32°. Beam hardening was reduced by the presence of a 0.5 mm Al-filter between the source and the detector. The raw data were reconstructed into two-dimensional slice images using Bruker's NRecon software. Corrections for the beam-hardening effect and ring artefacts were also applied during the reconstruction process. µ-CT datasets were visualized using Bruker's CTVox software.

Focused Ion beam and Transmission Electron Microscopy

Conventional X-ray studies on the new $Al_{52}Cu_{31}Fe_{10}Si_7$ approximant could not be carried out because of the small crystal size and its intergrowth with stolperite. For this reason, the FIB-TEM technique was applied. In preparation for the study with TEM, a thin lamella from the micrometeorite (Fig. 6) was prepared by FIB cutting using a Helios NanoLab G3 UC dual-beam FIB/SEM system. Sample thinning was accomplished by gently polishing the sample using a 2-kV gallium ion beam to minimize surface damage caused by the high-energy FIB. Conventional TEM imaging, selected area electron diffraction (SAED), atomic-resolution HAADF-

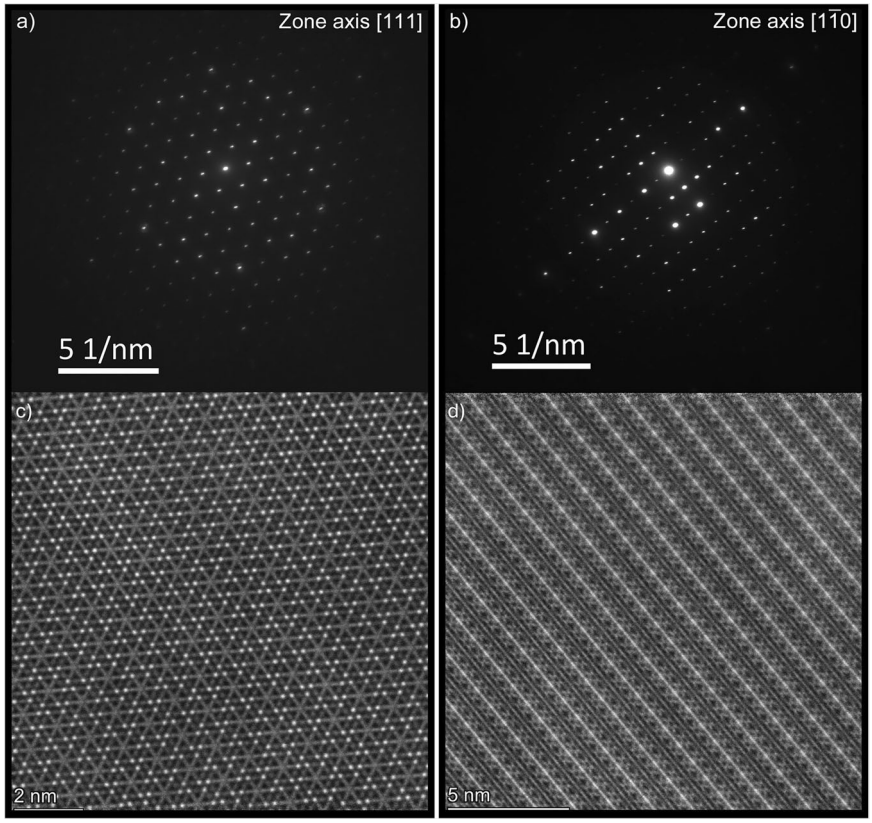

Fig. 9 | TEM analyses of FIB lamella. a SAED pattern taken on the red point shown in Fig. 8a) indicating a cubic symmetry with $a \approx 12.3$ Å. Zone axis [111]; **b** SAED pattern taken on the red point shown in Fig. 8a). Zone axis [1-10]. **c** HAADF-STEM image corresponding to SAED pattern shown in Fig. 9a). **d** HAADF-STEM image corresponding to SAED pattern shown in Fig. 9b). Note the periodicity across the field of view.

STEM imaging, and energy-dispersive X-ray spectroscopy (EDS) mapping (Fig. 7) were performed on a Titan Cubed Themis 300 double Cs-corrected STEM equipped with an extreme field emission gun source operated at 300 kV with a super-X EDS system. SAED patterns coming from the homogeneous region showing the $Al_{52}Cu_{31}Fe_{10}Si_7$ stoichiometry (Fig. 8a) can be indexed with the *Pm*-3 structure[23].

Secondary Ion Mass Spectrometry

Oxygen isotope analyses were carried out using a CAMECA IMS 1270 E7 at the Centre de Recherches Pétrographiques et Géochimiques (Nancy, France). $^{16}O-$, $^{17}O-$, and $^{18}O-$ ions produced by a Cs^+ primary ion beam (~10 µm and ~2 nA) were detected in multicollection mode using two off-axis Faraday cups (FCs) for $^{16}O-$ and $^{18}O-$ and the axial FC for $^{17}O-$. To remove the $^{16}OH-$ interference on the $^{17}O-$ peak and to obtain maximum flatness on the top of the $^{16}O-$ and $^{18}O-$ peaks, entrance and exit slits were adjusted to acquire a mass resolving power (MRP) of ≈7000 for $^{17}O-$ on the central FC. The multicollection FCs were set on slit 1 (MRP = 2500). The total measurement time was 180 s (150-s measurement + 30-s pre-sputtering). We used four in-house terrestrial standard materials (SCOL San Carlos olivine, CAF magnetite, BHVO basaltic glass, and JV1 diopside) to (i) define the instrumental mass fractionation line for the three oxygen isotopes and (ii) to correct the instrumental mass fractionation due to the matrix effect in samples. Typical count rates obtained on the San Carlos olivine standard were 1.7×10^9 cps for ^{16}O, 6.5×10^5 cps for ^{17}O, and 3.5×10^6 cps for ^{18}O. The 2σ errors were ≈0.25‰ for $\delta^{18}O$, ≈0.35‰ for $\delta^{17}O$, and ≈0.4‰ for $\Delta^{17}O$ ($\Delta^{17}O$ representing the deviation from the TFL, $\Delta^{17}O = \delta^{17}O - 0.52 \times \delta^{18}O$).

Data availability

Data presented in the paper can be accessed via figshare at: https://figshare.com/s/32eebc9e1f269367ebfb.

Received: 8 November 2024; Accepted: 25 March 2025;
Published online: 08 April 2025

References

1. Bindi, L., Steinhardt, P. J., Yao, N. & Lu, P. J. Natural Quasicrystals. *Science* **324**, 1306–1309 (2009).
2. Bindi, L. et al. Evidence for the extra-terrestrial origin of a natural quasicrystal. *Proc. Nat. Acad. Sci.* **109**, 1396–1401 (2012).
3. Steinhardt, P. J. & Bindi, L. In search of natural quasicrystals. *Rep. Prog. Phys.* **75**, 092601 (2012).
4. MacPherson, G. et al. Khatyrka, a new CV3 find from the Koryak Mountains, Eastern Russia. *Met. Plan. Sci.* **48**, 1499–1514 (2013).
5. Hollister, L. S. et al. Impact-induced shock and the formation of natural quasicrystals in the early Solar system. *Nat. Comm.* **5**, 4040 (2014).
6. Lin, C. et al. Evidence of redox reaction in the quasicrystal-bearing Khatyrka meteorite reveals multi-stage formation process. *Sci. Rep.* **7**, 1637 (2017).
7. Meier, M. M. M. et al. Cosmic history and a candidate parent asteroid for the quasicrystal-bearing meteorite Khatyrka. *Earth Plan. Sci. Lett.* **490**, 122–131 (2018).
8. Tommasini, S. et al. Trace elements conundrum of natural quasicrystals. *ACS Earth Space Chem.* **5**, 676–689 (2021).
9. Bindi, L., Steinhardt, P. J., Yao, N. & Lu, P. J. Icosahedrite, $Al_{63}Cu_{24}Fe_{13}$, the first natural quasicrystal. *Am. Mineral.* **96**, 928–931 (2011).
10. Bindi, L. et al. Natural quasicrystal with decagonal symmetry. *Sci. Rep.* **5**, 9111 (2015).
11. Bindi, L. et al. Decagonite, $Al_{71}Ni_{24}Fe_5$, a quasicrystal with decagonal symmetry from the Khatyrka CV3 carbonaceous chondrite. *Am. Mineral.* **100**, 2340–2343 (2015).
12. Bindi, L. et al. Collisions in outer space produced an icosahedral phase in the Khatyrka meteorite never observed previously in the laboratory. *Sci. Rep.* **6**, 38117 (2016).
13. Hu, J. et al. First synthesis of a unique icosahedral phase from the Khatyrka meteorite by shock-recovery experiment. *IUCrJ.* **7**, 434–444 (2020).

14. Suttle, M. D. et al. A unique CO-like micrometeorite hosting an exotic Al-Cu-Fe-bearing assemblage – close affinities with the Khatyrka meteorite. *Sci. Rep.* **9**, 12426 (2019).
15. Ma, C. et al. Al-Cu-Fe alloys in the solar system: Going inside a Khatyrka-like micrometeorite (KT01) from the Nubian desert, Sudan. *Met. Plan. Sci.* **58**, 1642–1653 (2023).
16. Genge, M. J. et al. The first Al-Cu-alloy-bearing unmelted micrometeorite suggests contributions from the disrupted ureilite protoplanet. *Earth Plan. Sci. Lett.* **656**, 119276 (2025).
17. Manzari, P., Mele, D., Tempesta, G. & Agrosì, G. New insights on the porosity and grain features of Al Haggounia 001, an impact-melt meteorite. *Lithos* **438-439**, 107015 (2023).
18. Agrosì, G. et al. Multiphase inclusions associated with residual carbonate in a transition zone diamond from Juina (Brazil). *Lithos* **350–351**, 105279 (2019).
19. Genge, M. J. et al. The classification of micrometeorites. *Met. Plan. Sci.* **43**, 497–515 (2008).
20. Genge, M. J., Grady, M. M. & Hutchison, R. The textures and compositions of fine-grained Antarctic micrometeorites: Implications for comparisons with meteorites. *Geoch. Cosmoch. Acta* **61**, 5149–5162 (1997).
21. Genge, M. J. et al. The mineralogy and petrology of I-type cosmic spherules: Implications for their sources, origins and identification in sedimentary rocks. *Geoch. Cosmoch. Acta* **218**, 167–200 (2017).
22. Genge, M. J. & Grady, M. M. The fusion crusts of stony meteorites: Implications for the atmospheric reprocessing of extraterrestrial materials. *Meteorit. Planet. Sci.* **34**, 341–356 (1999).
23. van Ginneken, M. et al. The identification of airbursts in the past: Insights from the BIT-58 layer. *Earth Plan. Sci. Lett.* **627**, 118562 (2024).
24. Genge, M. J. et al. The Fusion Crust of the Winchcombe Meteorite: Vigorous Degassing During Atmospheric Entry. *LPI Contrib.* **2695**, 6345 (2022).
25. Toppani, A., Libourel, G., Engrand, C. & Maurette, M. Experimental simulation of atmospheric entry of micrometeorites. *Met. Plan. Sci.* **36**, 1377–1396 (2001).
26. Quivy, A. et al. A cubic approximant of the icosahedral phase in the (Al-Si)-Cu-Fe. *Syst. J. Phys. Cond. Matter* **8**, 4223–4234 (1996).
27. Stadnik, Z. M. et al. Structural, Mössbauer, and transport studies of the icosahedral quasicrystals $Al_{55}Si_7Cu_{25.5}Fe_{12.5}$, $Al_{62.5}Cu_{24.5}Fe_{13}$ and the crystalline 1/1 approximant $Al_{55}Si_7Cu_{25.5}Fe_{12.5}$. *J. Phys. Cond. Matter* **15**, 6365–6380 (2003).
28. Puyraimond, F. et al. Atomic structure of the (Al, Si)CuFe cubic approximant phase. *Acta Cryst.* **A58**, 391–403 (2002).
29. Mitka, M. et al. Synthesis and stability of quasicrystalline phase in Al-Cu-Fe-Si mechanically alloyed powders. *J. Mater. Sci.* **56**, 11071–11082 (2021).
30. Bindi, L., Pham, J. & Steinhardt, P. J. Previously unknown quasicrystal periodic approximant found in space. *Sci. Rep.* **8**, 16271 (2018).
31. Bindi L. et al. Discovery of an Earthborn quasicrystal approximant. *Am. Mineral*. **110**, 650–654 (2025).
32. Asimow, P. D. et al. Shock synthesis of quasicrystals with implications for their origin in asteroid collisions. *Proc. Nat. Acad. Sci.* **113**, 7077–7081 (2016).
33. Oppenheim, J. et al. Shock synthesis of five-component icosahedral quasicrystals. *Sci. Rep.* **7**, 15629 (2017).
34. Folco, L. & Cordier, C. "Micrometeorites", Planetary Mineralogy, M. R. Lee, H. Leroux https://doi.org/10.1180/EMU-notes.15.9 (2015).

Acknowledgements

The authors thank Francesco Badolato for providing the micrometeorite. The authors are also very grateful to Nicola Mongelli for the SEM-analyses performed at the University of Bari (Italy). Bruker Skyscan 1172 high-resolution μX-CT scanner has been purchased with funds from "PON Ricerca e Competitività 2007–2013". This study was also conducted within the Space It Up project funded by the Italian Space Agency, ASI, and the Ministry of University and Research, MUR, under contract n. 2024-5-E.0-CUP n. I53D24000060005. The authors acknowledge the use of Princeton's Imaging and Analysis Centre, which is partially supported by the Princeton Centre for Complex Materials, a National Science Foundation (NSF)-MRSEC programme (DMR-2011750).

Author contributions

G.A., P.M., G.T. and F.R. did the preliminary SEM characterization of the sample. D.M. carried out the micro-computed X-ray tomography study. T.C. performed the SEM and EBSD studies on the polished section of the spherule. G.C. and N.Y. carried out the FIB-TEM study. J.V. did the oxygen isotope analysis. G.A. and L.B. wrote the manuscript. All authors discussed the results and commented on the manuscript.

Competing interests

The authors declare no competing interests.

Additional information

Supplementary information The online version contains supplementary material available at https://doi.org/10.1038/s43247-025-02245-w.

Correspondence and requests for materials should be addressed to Giovanna Agrosì or Luca Bindi.

Peer review information *Communications Earth & Environment* thanks Rick Hugo, Carlos Pina and the other, anonymous, reviewer(s) for their contribution to the peer review of this work. Primary Handling Editor: Joe Aslin. A peer review file is available.